Journal of Data Acquisition and Processing
ISSN: 1004-9037
https://sjcjycl.cn/
DOI: 10.5281/zenodo.7765924

# DOUBLE DIFFUSIVE EFFECTS ON MAXWELL-NANO FLUID CHEMICALLY REACTING FLOW GENERATED BY STRETCHING A SHEET ACROSS A POROUS MEDIUM WITH MHD

**R. S. DurgaRao*, R. Vijayakumar[1] and V. Vasudeva Murthy[2]**
*Department of Mathematics, Vishnu Institute of Technology, Bhimavaram, West Godavari(Dt), 534201, Andhra Pradesh, India
Email: durgarao.r@vishnu.edu.in
[1]Mathematics Section, FEAT, Annamalai University, Chidambaram, Tamil nadu State, India| Department of Mathematics, Periyar Government Arts College, Cuddalore, 607001, Tamil nadu State, India
[2]Department of Mathematics, S.R.K.R. Engineering College, Bhimavaram, West Godavari (Dt), 534201, Andhra Pradesh, India
**[1]Corresponding author Email address: rathirath_viji@yahoo.co.in**

**Abstract:** This study aims to elucidate Nano fluid Maxwell non-Newtonian slip flow phenomenon caused by a stretched sheet implanted with an abrasive surface and sensitive to chemical and magnetic processes. The energy equation is used to investigate of thermophoresis and Brownian motion's influence. The fundamental flow controlling equations can be converted into a dimensionless for mutilising similarity transformation. The Runge-Kutta method and firing strategy have been utilised to quantitatively solve these dimensionless issues. The primary goals of the current study are to investigate important variables that are included in the governing equations and their visual effects on distributions of temperature concentrations, and velocity. A graphic demonstrates the consistency of the most recent findings. Additionally provided The significance of the Coefficients of Skin-Friction, Nusselt number, and Sherwood number are shown in a table. The scope of the current inquiry findings as well as the published benchmark, which illustrates a unique circumstance, are in good agreement.

**Keywords:** Maxwell fluid; Nanofluid; MHD; Porous medium; Double diffusion; Chemical reaction; Stretching sheet;

## Nomenclature

### List of Symbols

$u, v$: Velocity components in the directions of x and $y(m/s)$

$x, y$: Along the stretching sheet Calculated Cartesian coordinates $(m)$

$f$ : Dimensionality-free flow function

$f'$ : velocity of the Fluid$(m/s)$

Pr: Prandtl number

$C$ : Fluid nanoparticle volume concentration $(mol/m^3)$

$T$ : Fluid temperature $(K)$

$O$ : Origin

$C_\infty$ : Dimensional ambient volume fraction $(mol/m^3)$

$C_w$: Concentration of nanoparticle dimensions at the stretching surface $(mol/m^3)$

$T_w$: Temperature of the nanofluid near wall$(K)$

$B_o$: Constant magnetic field $(Tesla)$

$M$: Parameter of Magnetic field

$T_\infty$: From the stretching sheet $(K)$ Temperature of the liquid distant

$Cf$ : Coefficient of skin friction $(s^{-1})$

$Nb$ : Parameter Brownian motion

$U_w$: Fluid Stretching velocity$(m/s)$

$Nu$: Heat transfer rate coefficient (or)Nusselt number

$Nt$: Thermophoresis parameter

$Sc$: Schmidt number

$q_w$: Heat flux coefficient

$q_m$: Coefficient Mass flux coefficient

$C_p$: Nano particles Specific heat capacity $(J/kg/K)$

$D_B$: The coefficient Brownian diffusion

$D_T$: Coefficient of Thermophoresis diffusion$(m^2/s)$

$Sh$: The Coefficient rate of Mass transfer (or) Sherwood number

$K$: Parameter of Permeability$(m^{-1})$

$k_1$: Porous medium Permeability $(m^{-1})$

$a$: Positive real number

$\mathrm{Re}_x$: Reynold's number

$Du$: Dufour number

$Sr$: Soret number

$C_s$: Concentration susceptibility

$k_r$: DimensionalParameter of chemical reaction

$Kr$: Dimensional Parameter of chemical reaction

$K_T$: The ratio of thermal diffusion

$D_m$: Solutal diffusivity of the medium

$T_m$: Fluid Mean temperature

### Greek symbols

$\eta$: Non-**Dimensional**similarVariable $(m)$

$\theta$ :Temperature that is not dimensioned $(K)$

$\phi$ :Nanoparticle concentration that is not dimensioned $(mol/m^3)$

$\alpha_m$: Heat diffusivity, $(m^2/s)$

$\nu$: The kinematic viscosity, $(m^2/s)$

$\sigma$ : Electrical conductivity

$\rho$ : The fluid 's Density, $(kg/m^3)$

$\mu$ : Fluid 's dynamic viscosity,

$\kappa$ : Fluid Thermal conductivity $(W/(m.K))$

$\beta$ : Maxwell parameter of fluid

$\psi$ : Stream function

$\beta_1$ : Time relaxation of the fluid

$\tau_B$ : Cauchy Stress tensor

$\tau_w$ : Shear stress

**Superscript**

$'$ : Derivable about to $\eta$

**Subscripts**

$f$ : Fluid,

$w$ : The state of the sheet,

$\infty$ : Ambient Conditions.

## 1. Introduction:

The Soret effect relates to mass flux phenomena generated via thermal conduction, whereas the Dufour effect relates to energy flow induced by chemical difference. The effect of Soret is utilised when dealing with gaseous concentrations that have lighter and middle molecular weight weights. The Dufour and Soret phenomena are used to transfer mass and heat in many engineering and industrial applications, including multi-component melts in geosciences, groundwater contamination movement, The crystallisation binaries alloys, Oil reservoirs, Chemical reactors, as well as space cooling, and isotopic distinction, and gas mixes. [1]. Bekezhanova and Goncharova [2] looked at how the aggregate actions of Soret and Dufouraltered the properties ofthe fluid's flowthat was evaporating. Sallesh et al. [3] showed the combined impacts of Soretand Dufour on the flow of forced convection in the direction of a thin needle in motion utilising the The nanofluid model Buongiorno. Jawad et al. [4] studied on MHDboundary layer.The Soret was coupled via a Darcy-Forchheimer nanofluid flow., Dufour, and impacts to the convection of Marangoni. The fluid dynamics of spinning disc Soret-Dufour collisions in both uphill and downhill orientations were studied by Shehzad et al. [5]. Olanrewaju and Makinde [6] looked at the impact softhermal diffusionand the impact of diffusion thermo on the transmission of mass andheat through a vertically revolving plate with suction/injection through a MHD boundary layer by chemically reacting. The components for heat transmission, chemical reaction, and ferrofluid motion are found in the Maxwell's boundary layer, according to investigations by Majeed et al. [7], which also looked at the effectsof Soret and suction. Reddy and Chamkha [8] examined the effectsof Dufourand Soret on unstable Magneto hydro dynamics heat and mass transport through a porous material, Thermophoresis and nonuniform heat production/absorption in a stretched sheet.Yinusa[9] researched the crushed stream, heat exchange, and mass transfer three-dimensional via a twisting tube to account for both the effects of Dufour and Soret. Khan et al. [10] using the finite difference approach to verify the impactsof Dufour and Soret as well as the influence of viscous fluid on the increase in entropy. Venkatesh et al. [11] looked at the joint effects of the Dufour and Soret on Maxwell fluid flow of the MHD boundary layer on a stretched sheet containing nanoparticles. Siva Reddy Sheri and R. Srinivasa Raju examined Soret's effect on unstable MHD free convection over a semi-infinite vertical plate with viscous dissipation. [12]. Anand Rao et al. [13] investigated using The finite element approach is used to simulate the unstable Soret, Dufour, thermal radiation, and a heat source govern MHD free convection flow

across an infinite vertical plate. Okuyade et al. [14] used heat radiation to analyse on a vertical plate the fluctuating MHD free convective fluid flows. Motsa and Shateyi[15] applied the successive linearization strategy on partial slip, impactsof thermal diffusion, and diffusion-thermo for consistent convective flow with MHD caused by a rotating disc. Sardar et al. [16] verifiedin the Soret and Dufour presence influences a wedge-shaped mixed convection Carreau nanofluid flow. Sharada and Shankar [17] looked at the impact of Dufour and Soret over an exponentially stretched sheet with concentration slip on the Carreau nanofluid MHD mixed convection flow. Ahmad et al[18]using the non-polynomial cubic spline approachby using method of the finite element the numerical resolutionfound four parabolic homogeneous partial differential equations, Ali et al. [19] evaluated theimpacts of Soret and Dufour on MHD rotational Oldroyd-B nanofluid flows across a a sheet stretched with coupled diffusion Cattaneo-Christov model of heat flow. Srinivasacharya et al. [20] analysed the effect of the of Dufour and Soret on the basis of mixed convectionon a vertical, undulating in a porous materialsurface with a variety of properties. In their study [21], Shojaei et al. with Dufour and Soret impactsdiscussed the hydrothermal investigation second-order non-Newtonian radiative stretching cylinder's fluid flow. Pal and Mondal [22] investigated through the effect of thermophoresis and Soret-Dufour on themass and heat transport in a non-isothermal wedge that radiates heat and dissipates it. Makinde [23] examined the influence Soret and Dufour's work on MHD mixed convection flow using a vertical plate immersed in a porous plate medium. When radiative heat transmission and an irreversible chemical process of the nth order are present, Makinde and Olanrewaju[24] exploredthrough a binary mixture the unstable mixed convection of the flow. It is believed if the fluid is thin visually. The contributions made by Soret and Dufour to numerous academic subjects were examined in several of the research projects ([25]-[35]).

The major objective of this inquiry is to evaluate the interaction between diffusion thermo and thermal diffusion to influence the fluid flowof Maxwell in the MHD the border layer of the presence of a porous medium containing nanofluid particles through a stretched sheet. The cornerstone of our inquiry is laid forth in the aforementioned reference documents. By applying the Runge-Kutta and the shooting methods the basic corresponding equations for this inquiry were solved. The Maxwell fluid parameter (β), the Soret number (Sr), the Dufour number (Du), , the Prandtl number (Pr), the parameter of Thermophoresis (Nt), the parameter of Brownian motion (Nb),the Permeability parameter (K), , the Schmidt number (Sc), the Chemical reaction cooefficient (Kr), and the Magnetic parameter will all be graphically illustrated in this study to show how they affect concentration, temperature, and velocity profiles (M). Nusselt, Sherwoodthe Skin-friction, numbers' numerical values are also shown and discussed using table forms. This work's the following is the structure Section 2 includes a description of governing linked nonlinear ordinary dirivible equations. Section 3 goes into great detail on the evolution of the Runge-Kutta approach and a shooting method in order to resolve the governing equations. Section 4 goes into great detail about the code checking for the programme. Section 5 presents the findings and observations. Results are detailed in further detail in Section 6.

## 2. Flow Governing Equations

This section examines, on two-dimensional thermal diffusion and thermodynamic diffusion influence, viscous, steady, incompressible, conductive electrically Maxwell fluid flow under the presence of a magnetic field towards a stretching sheet, chemical reaction and porous medium impacts including thermophoresis and Brownian motion. The geometry of the flow of this investigation is shown in

Fig. 1. The given hypotheses are developed for this analysis:

i. The coordinate axes used are the major axis parallel to the direction of flow and minor axis normal to flow direction, as demonstrated in Figure 1

ii. Stretchedplate with a velocity Uw = ax, along x-axis where stretching parametera >0 .

iii. Boundary layer occurs at the normal coordinate specified for the stretching surface at $y \geq 0$

iv. Moreover, also considered are the chemical interaction with effects of thermophoresis and Brownian motion

v. Surface temperature at with Tw and far away the surface as T∞ are symbolized. The symbols are Cw and C∞ for concentration respectively.

vi. The influence of a uniform magnetic field of strength Bo, steady and convective Maxwell-flow of nanofluid with a boundary layer is seen

vii. By the produced magnetic field is regarded as trivial. The magnetic Reynolds number is thought to be negligible;

viii. Moreover, The preceding assumptions let the Joule heating, viscous dissipation, and body forces to be disregarded.

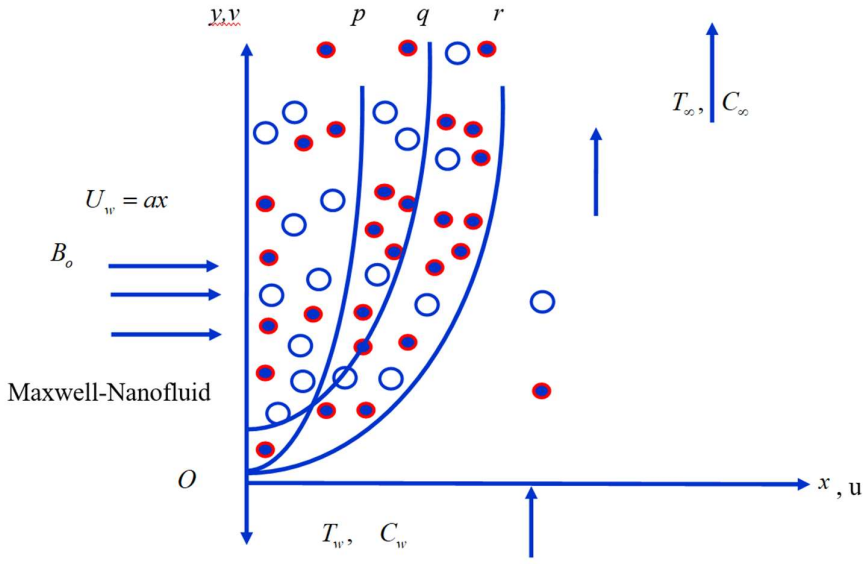


*p* ---- Momentum boundarylayer, *q*---- Thermal boundarylayer & *r*---- Concentration boundarylayer

Fig. 1.:Geometrical expression of the fluid

the basic equations governing flow for steady, two-dimensional, electrically conducting, incompressible, on the basis of above assumptions, Maxwell-nanofluid flow are:

*Continuity Equation:*

$$\frac{\partial u}{\partial x}+\frac{\partial v}{\partial y}=0, \quad (1)$$

*Momentum Equation:*

$$u\frac{\partial u}{\partial x}+v\frac{\partial u}{\partial y}=\nu\frac{\partial^2 u}{\partial y^2}-\beta_1\left(u^2\frac{\partial^2 u}{\partial x^2}+2uv\frac{\partial^2 u}{\partial x\partial y}+v^2\frac{\partial^2 u}{\partial y^2}\right)-\frac{\sigma B_o^2}{\rho}\left(u+\beta_1 v\frac{\partial u}{\partial y}\right)-\nu\left(\frac{u}{k_1}\right), \quad (2)$$

*Equation of thermal energy:*

$$u\frac{\partial T}{\partial x}+v\frac{\partial T}{\partial y}=\alpha_m\frac{\partial^2 T}{\partial y^2}+\tau_B\left\{D_B\frac{\partial C}{\partial y}\frac{\partial T}{\partial y}+\frac{D_T}{T_\infty}\left(\frac{\partial T}{\partial y}\right)^2\right\}+\frac{D_m K_T}{C_s C_p}\left(\frac{\partial^2 C}{\partial y^2}\right), \quad (3)$$

*Equation of species nanoparticle volume concentration:*

$$u\frac{\partial C}{\partial x}+v\frac{\partial C}{\partial y}=D_B\frac{\partial^2 C}{\partial y^2}+\frac{D_T}{T_\infty}\frac{\partial^2 T}{\partial y^2}-k_r\left(C-C_\infty\right)+\frac{D_m K_T}{T_m}\left(\frac{\partial^2 T}{\partial y^2}\right), \quad (4)$$

The flow's boundary conditions are:

$$\left.\begin{aligned}&u=U_w(x)=ax,\ T=T_w,\ C=C_w \ \ at \ \ y=0\\&u\to 0,\ T\to T_\infty,\ C\to C_\infty \ \ as \ \ y\to\infty\end{aligned}\right\} \quad (5)$$

The governing equations are transformed into ordinary differential equations with the similarity transformation given below,

$$\left.\begin{aligned}&u=axf'(\eta),\ v=-\sqrt{a\nu}f(\eta),\ \eta=y\sqrt{\frac{a}{\nu}},\ \ \theta=\frac{T-T_\infty}{T_w-T_\infty},\ \phi=\frac{C-C_\infty}{C_w-C_\infty}\end{aligned}\right\}, \quad (6)$$

Along withboundary conditions (5) the basic governing equations (2), (3) and (4) by usingthe similarity transformations (6), take the following forms:

$$f'''+ff''-\left(f'^2\right)+\beta\left(2ff'f''-f^2f'''\right)-\left(M+K\right)f'+M\beta f\,f''=0, \quad (7)$$

$$\theta''+\Pr f\theta'+\Pr Nb\theta'\phi'+\Pr Nt\theta'^2+\Pr Du\phi''=0, \quad (8)$$

$$Nb\phi''+NbScf\phi'+Nt\theta''-ScKr\phi+ScSrNb\theta''=0, \quad (9)$$

the associated boundary conditions (5) become

$$\left.\begin{aligned}&f'(0)=1,\ f(0)=0,\ \ \theta(0)=1,\ \ \phi(0)=1,\ f'(\infty)\to 0,\ \theta(\infty)\to 0,\ \ \phi(\infty)\to 0\end{aligned}\right\}, \quad (10)$$

where the physical parameters involved are stated as

$$\left.\begin{aligned}&M=\frac{\sigma B_o^2}{\rho a},\ \ K=\frac{\nu}{ak_1},\ \Pr=\frac{\nu}{\alpha_m},\ Nb=\frac{\tau_B D_B\left(C_w-C_\infty\right)}{\nu},\ \ \beta=\beta_1 a,\ Kr=\frac{k_r}{a},\\&Sc=\frac{\nu}{D_B},\ \ Nt=\frac{\tau_B D_T\left(T_\infty-T_m\right)}{\nu T_\infty},\ Sr=\frac{D_m K_T(T_w-T_\infty)}{T_m\nu\left(C_w-C_\infty\right)},\ \ Du=\frac{D_m K_T\left(C_w-C_\infty\right)}{C_s C_p\nu\left(T-T_\infty\right)},\end{aligned}\right\}, \quad (11)$$

Significant physical quantities, such as the Skin-friction (Cf), the local Nusselt number (Nu), and the local Sherwood number (Sh),coefficients are showed as follows:

$$C_f=\frac{\tau_w}{\rho U_w^2}=\frac{1}{\rho U_w^2}\mu\left(\frac{\partial u}{\partial y}\right)_{y=0}\Rightarrow Cf=C_f\left(\sqrt{\mathrm{Re}_x}\right)=f''(0) \quad (12)$$

$$Nu_x = \frac{xq_w}{\kappa\left(T_w - T_\infty\right)} = -\frac{x\kappa\left(\frac{\partial T}{\partial y}\right)_{y=0}}{\kappa\left(T_w - T_\infty\right)} \Rightarrow Nu = Nu_x\left(\mathrm{Re}_x\right)^{\frac{-1}{2}} = -\theta'(0) \quad (13)$$

$$Sh_x = \frac{xq_m}{D_B\left(C_w - C_\infty\right)} = -\frac{D_B\left(\frac{\partial C}{\partial y}\right)_{y=0}}{\left(C_w - C_\infty\right)} \Rightarrow Sh = Sh_x\left(\mathrm{Re}_x\right)^{\frac{-1}{2}} = -\phi'(0) \quad (14)$$

## 3. Solution Methodby Runge-Kutta method:

In the event of a complete set of Eqs. (7)-(9), it does not appear that an accurate solution is available (9). This is because (7)-(9) are nonlinear, with adequate boundary conditions supplied by Equation (10) and the necessity for problem-solving using numerical approaches: Using Similarity modifications, the controlling differential equations with partial solutions are transformed into a collection of nonlinear ordinary differential equations that may be numerically solved. The shooting approach is utilised in conjunction with strategy of the method of fourth-order Runge-Kutta to numerically solve the ensuing boundary value problem. A group of differential equations first-order is generated by reducing nonlinear differential equations to first-order diriveble equations. The linked ordinary differentiable equations (7)-(9) have been diminished, as depicted, to a group of containing seven unknowns 7 simultaneous equations with 7 unknowns. The interconnected standard differential equations. (7)-(9) are third order in $f(\eta)$ and second order in $\theta(\eta)$ and $\phi(\eta)$ which have been simplified containing seven unknowns in seven concurrent equations. Seven initial conditions are required to solve by numerically this system of equations using the Runge-Kutta method., however both the initial conditions are sufficient in $f(\eta)$ one initial condition in each of $\theta(\eta)$ and $\phi(\eta)$ are known. However, the values of $f'(\eta)$,$\theta(\eta)$ and $\phi(\eta)$ are known at $\eta \to \infty$. Using the shooting procedure, these final conditions are applied to generate unknown beginning conditions at $\eta = 0$. The most crucial stage of this method determines the best discrete value of. To estimate the value, we begin with a wild guess and work our way through the boundary value issue with the provided variables. of eqs. (7)-(9) toget $f''(0), \theta'(0)$ and $\phi'(0)$. With an additional higher value of $\eta_\infty$ the method of the procedure is done until two consecutive values of $f''(0), \theta'(0)$ and $\phi'(0)$ vary only after the significant digit selected. The final result $\eta_\infty$is utilised as the finite limit $\eta_\infty$ for the specific collection of physical parameters used to determine velocity, temperature, and concentration, respectively, are$f(\eta)$, $\theta(\eta)$ and $\phi(\eta)$ in the boundary layer. After obtaining the initial conditions, integration is used to solve this group of simultaneous equations. strategy of Runge-Kutta the fourth order. In order to prevent numerical oscillation, the value is adjusted at 8 based on the physical characteristics that influence the flow. In consequence, the associated boundary value problem of third-order in $f(\eta)$, second-order in $\theta(\eta)$ and $\phi(\eta)$ has been simplified to seven first-order simultaneous equations for seven unknowns

$$\left.\begin{aligned} & f' = p \Rightarrow f'' = p' = q \Rightarrow f''' = p'' = q' \Rightarrow q' = \frac{Mp + Kp + p^2 - fq - 2\beta fpq - M\beta fq}{\left(1 - \beta f^2\right)} \\ & \theta' = r \Rightarrow \theta'' = r' \text{ then } r' = -\left(\mathrm{Pr}\right) fr - \left(\mathrm{Pr}\right)\left(Nb\right) rz - \left(\mathrm{Pr}\right)\left(Nt\right) r^2 - \left(\mathrm{Pr}\right)\left(Du\right) z' \\ & \& \\ & \phi' = z \Rightarrow \phi'' = z' \text{ then } Nbz' = -\left(Sc\right)\left(Nb\right) fz - \left(Nt\right) r' + \left(Sc\right)\left(Kr\right)\phi - \left(Sc\right)\left(Sr\right)\left(Nb\right) r' \end{aligned}\right\} \quad (15)$$

the associated limit conditions became

$$p(0)=1,\ f(0)=0,\ \theta(0)=1,\ \phi(0)=1,\ p(\infty)\to 0,\ \theta(\infty)\to 0,\ \phi(\infty)\to 0 \quad (16)$$

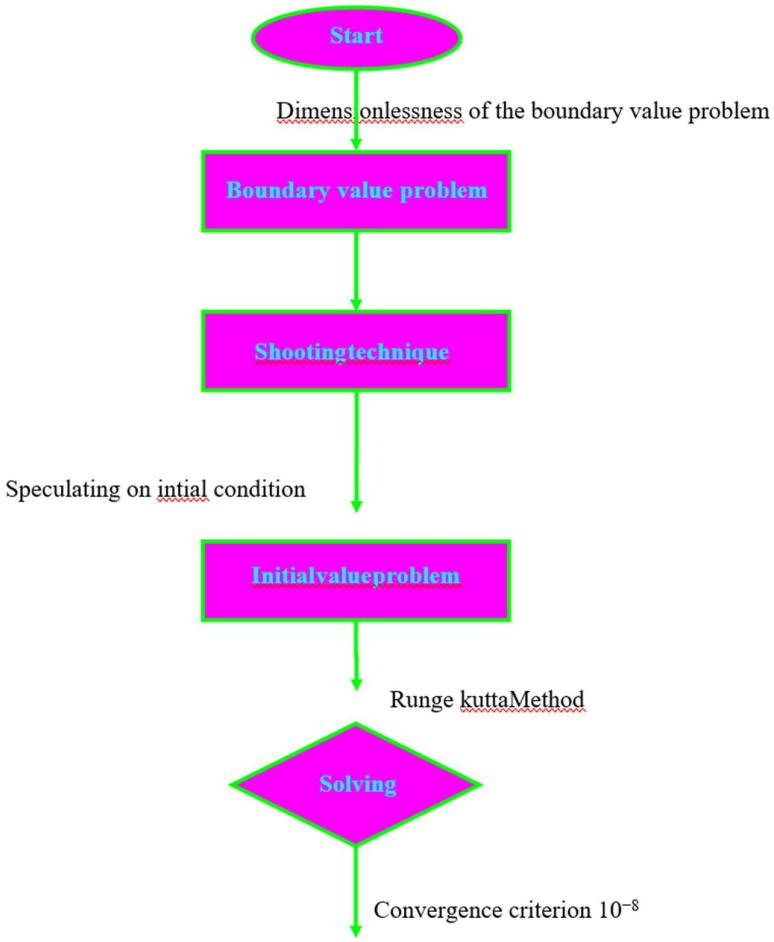


**Fig. 2.:** Numerical procedure Flow diagram

The problem of boundary value is initially turned into a problem of starting value (IVP), which is expanded upon investigated. After that, the initial value problem is handled by properly estimating missing beginning value for several factor combinations based on the shooting method are employed till the issue is resolved.. The step size here in y his scenarioh = 0.1 is utilised for calculations. In addition, a 10-6employing tolerancerror. The collected data is given in the form of tabular and graphs, with an in-depth examination of the issues' most prominent characteristics.

## 4. Program Code Validation:

Table-1.: Current rate of heat transmission (Nusselt number) coefficient data are compared to published results. of Makinde and Aziz [36] when $M = \beta = Nb = Nt = K = Kr = Sr = Du = 0$

| Pr | Nusselt number results of Makinde and Aziz [36] | Existing Nusselt number results |
|---|---|---|
| 0.070 | 0.0656 | 0.059678650987369873933869 8 |
| 0.200 | 0.1691 | 0.156783193846394834386938 4 |

| | | |
|---|---|---|
| 0.700 | 0.4539 | 0.4409010987690386798579851 |
| 2.000 | 0.9114 | 0.9098571863760379603109610 |
| 7.000 | 1.8954 | 1.8885775137376387630876387 |
| 20.00 | 3.3539 | 3.3456776848379631007367653 |
| 70.00 | 6.4622 | 6.4578810484198376459864962 |

From table-1, the authors have discussed the comparing current outcomes with published The analytical outcomes of Makinde and Aziz [36] for program code validation in absence of Magnetic field, Maxwell fluid, Porous medium, Thermophoresis, Brownian motion, Soret number, Chemical reaction and Dufour number effects. In this table, The current results demonstrate excellent concordance and coincide with the published results.

## 5. Discussion with Results :

In this part, the generated numerical solutions of the profiles of velocity, temperature, and concentrationare analysed using graphs for variations in distinct parameters physically, parameter of Magnetic field (M = 0.1, 0.3, 0.5, 0.8), Permeability parameter (K = 0.3, 0.5, 0.7, 1.0), Parameter of Maxwell fluid (β = 0.2, 0.4, 0.6, 1.0), Prandtl number (Pr = 0.71, 1.0, 3.0, 7.0), parameter Thermophoresis (Nt = 0.1, 0.3, 0.5, 0.7), Brownian motion parameter (Nb = 0.1, 0.2, 0.3, 0.4), Dufour number (Du = 0.5, 1.0, 1.5, 2.0), Soret number (Sr = 0.5, 1.0, 1.5, 2.0), Chemical reaction parameter (Kr = 0.5, 0.8, 1.2, 1.5) and Schmidt number (Sc = 0.22, 0.30, 0.60, 0.78) in figures 3, 4, 5, 6, 7, 8, 9, 10, 11, 12, 13, 14. Other parameters such as the coefficient of skin friction (Cf), Nusselt number (Nu) is the rate of heat transfer coefficient and Sherwood number (Sh) is the rate of mass transfer coefficient are also given numerical values discussed and expressed in tabular forms.

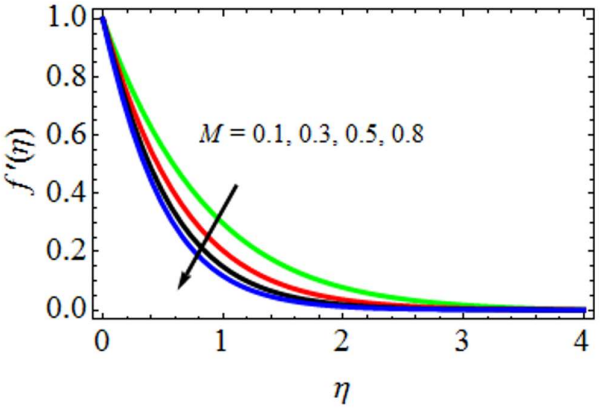


**Fig. 3.***M* effect on profiles of velocity

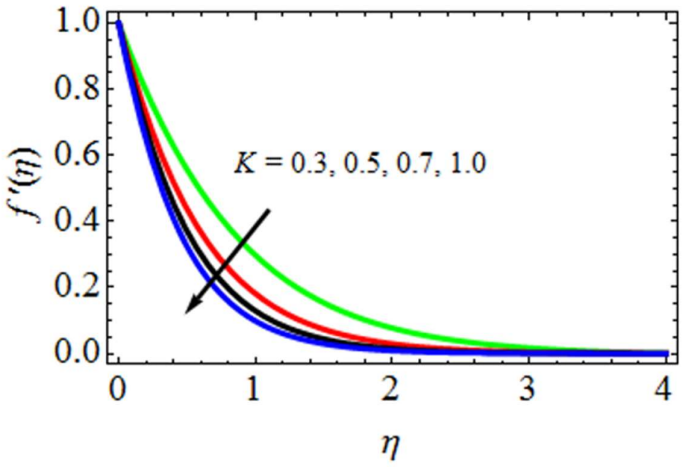


**Fig. 4.***K*impact on profiles of velocity

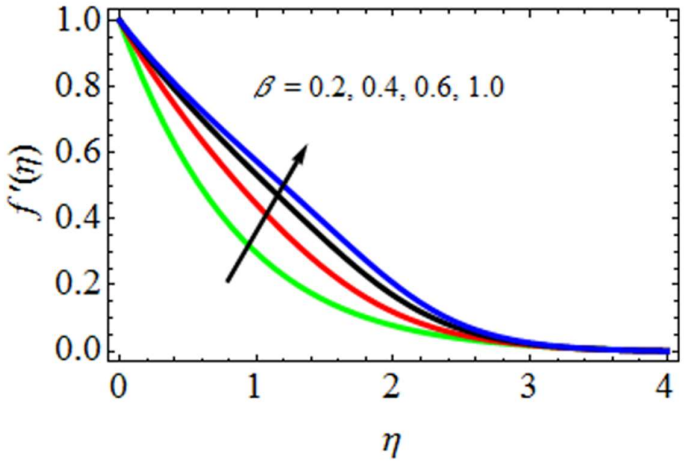


**Fig. 5.***β*impacton profiles of velocity

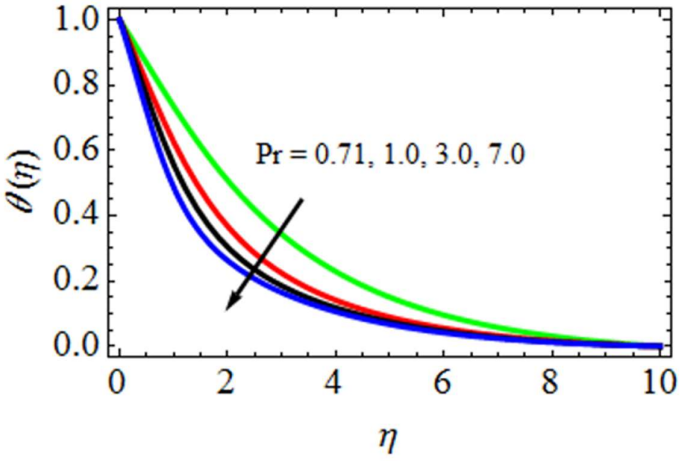


**Fig. 6.**Primpact on profiles of temperature

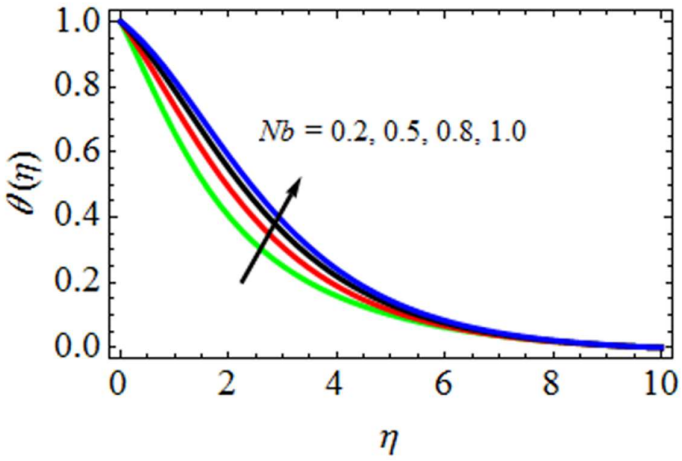


**Fig. 7.** *Nb* impact on profiles of temperature

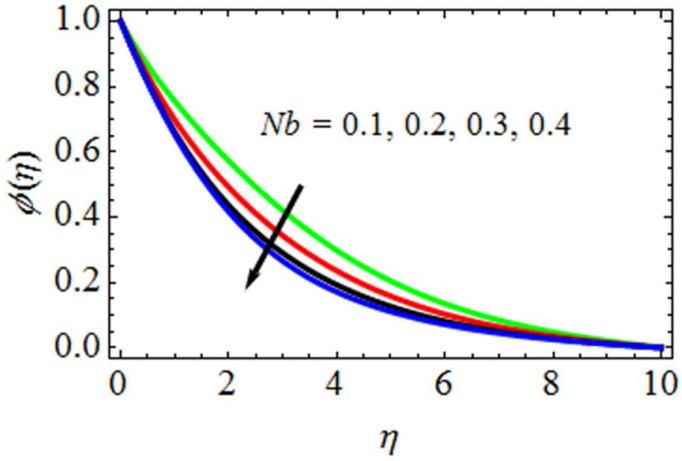


**Fig. 8.** *Nb* impact on profiles on concentration

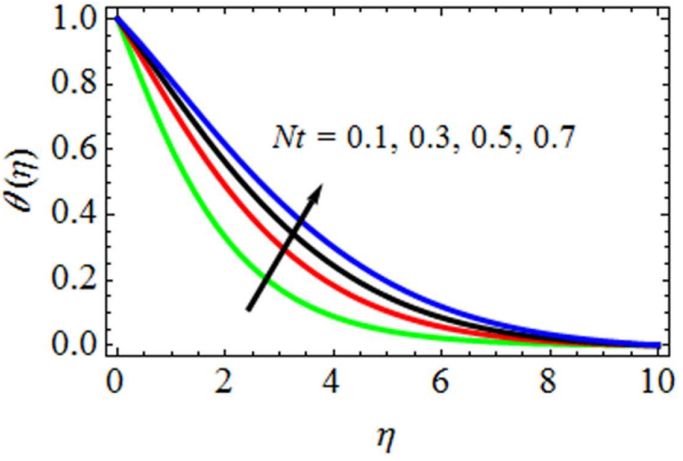


**Fig. 9.** *Nt* impact on profiles on temperature

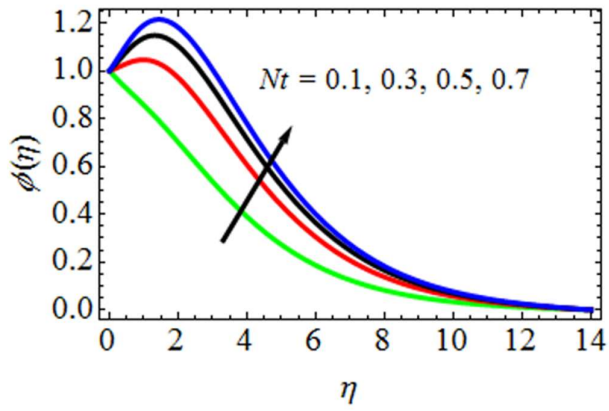


**Fig. 10.** *Nt* impact on profiles of concentration

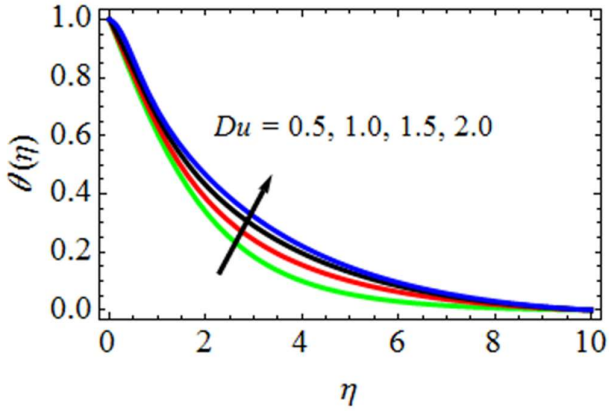


**Fig. 11.** *Du* impact on profiles of temperature

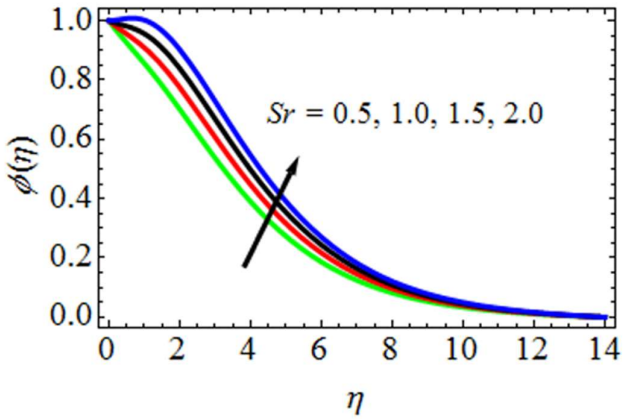


**Fig. 12.** *Sr* impact on profiles of concentration

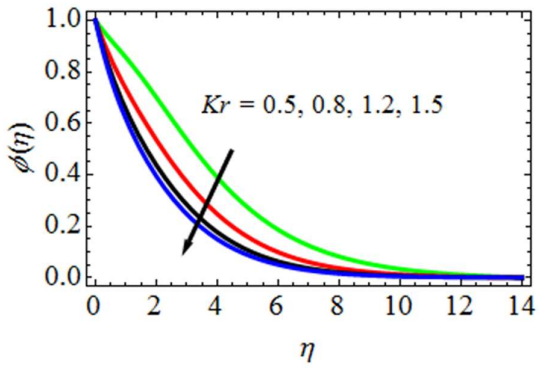


**Fig. 13.** *Kr* impact on profiles of concentration

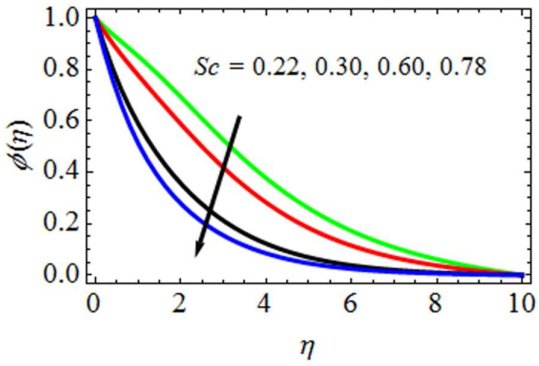


**Fig. 14.** *Sc* impact on profiles of concentration

Fig. 3 demonstrates the variations of parameter of Magnetic field(M = 0.1, 0.3, 0.5, 0.8) on stream wise velocity profiles. It has been discovered that there is an inverse link between magnetic parameter and velocity profiles along the stream. This is because, when The Lorentz force is created when the magnetic parameter rises. In opposition to the mobility of fluid particles, this force causes a resistive force through its generation. Hence, stream wise velocity is diminished..Fig. 4 demonstrates the effect of Permeability parameter (K = 0.3, 0.5, 0.7, 1.0) on profiles of velocity. It is obvious that the influence of porous material results in greater fluid flow restriction. Which therefore slows down the fluid's movement? Hence, when the permeability parameter increases, the fluid's resistance to motion increases, resulting in a reduction in velocity. Effect of Maxwell fluid parameter (β = 0.2, 0.4, 0.6, 1.0) physical parameters on the non-dimensional velocity profiles is discussed in Fig. 5. From this figure, it is seen that Maxwell fluid parameter increases when rise in the parametric values of the velocity profiles. Fig.6 illustrates impact of Prandtl Number (Pr = 0.71, 1.0, 3.0, 7.0). The profile of the temperature declines as the Prandtl number increases. Thermal diffusivity and the Prandtl parameter are inversely related. Greater estimates of the Prandtl value indicate in thermal diffusivity decrease, resulting in a reduction in temperature dispersion. A decrease in the Prandtl number reduces thermal diffusivity slows the diffusion of warmth and hence decreases the thermal sketch. The parameter of Brownian motion effect(Nb = 0.1, 0.2, 0.3, 0.4) on temperature and concentration profiles is shown in Figs. 7 and 8 respectively. By increasing the Brownian motion parameter, the temperature profile stabilised at higher levels. Brownian

motion is the random motion caused by nanoparticle collisions with the base fluid. The greater the parameter of Brownian motion, the greater the collision. Due to particle collisions, the fluid's internal kinetic energy rises. The Brownian motion and concentration profile have an inverse connection theparameter of Brownian motion more then the number of nanoparticles less in the base fluid. Figs. 9 and 10reveal the effect of thermophoresis parameter (Nt = 0.1, 0.3, 0.5, 0.7) on profiles of temperature and concentration. As Nt increases Profiles of Temperature and concentration both rise. Thermophoresis is the transport force resulting from the difference in temperature between fluid layers. More value Thermophoresis indicates thus the temperature disparity between the layers widens, hence increasing the rate of heat transformation. By increasing the nanoparticles, the fluid concentration rises. More nanoparticles result in a greater heat transition across layers, therefore Nt raises both temperature and concentration profiles.Fig. 11demonstrated that profile of the fluid temperature rises as the Dufour number (Du= 0.5, 1.0, 1.5, 2.0) increases. Physically, this phenomena may be defined as follows: if chemically non-reacting two separate fluids of the equal temperature are allowed to diffuse in a system, then the temperature differential between the fluids grows..The Soret number (Sr = 0.5, 1.0, 1.5, 2.0) effect on concentration profiles is shown in Fig. 12, and increases of fluid concentration it depicted that Soret number. Owing to the impacts of irreversible process The term "infrared spectroscopy" refers to the process of determining the wavelength of light. It has the potential to increase the flow system's concentration flux. This is presented in Fig. 12. The characteristic of Chemical reaction parameter (Kr = 0.5, 0.8, 1.2, 1.5) on concentration profiles are discussed in Fig. 13. The graph clearly demonstrates that, as the concentration profiles of the flow decrease when the chemical reaction parameter increases,..The variation of profiles of concentration ($\phi$) for the assessment of Schmidt number (Sc = 0.22, 0.30, 0.60, 0.78) can be calculated from Fig. 14. We can see that when the Schmidt number (Sc) increases, the concentration of nanoparticles decreases. The Schmidt number is calculated by dividing the relative thickness of the concentration and momentum boundary layers. When Sc is small, mass diffusion is more than the momentum. So,compared to the momentum boundary layer the concentration boundary layer is thicker. Table-2illustrates the numerical values of the skin-friction coefficient for variations in the values of technical factors such as the magnetic field parameter (M = 0.1, 0.3, 0.5), parameter of Permeability (K = 0.3, 0.5, 0.7), Maxwell fluid parameter ($\beta$ = 0.2, 0.4, 0.6), Prandtl number (Pr = 0.71, 1.0, 3.0), Thermophoresis parameter Nt = 0.1, 0.3, 0.5), parameter of Brownian motion (Nb = 0.1, 0.2, 0.3), Dufour number (Du = 0.5, 1.0, 1.5), Soret number (Sr = 0.5, 1.0, 1.5), Chemical reaction parameter (Kr = 0.5, 0.8, 1.2) and Schmidt number (Sc = 0.22, 0.30, 0.60). From this table, it is observed that with rising values ofThermophoresis parameter (Nt = 0.1, 0.3, 0.5), Brownian motion parameter (Nb = 0.1, 0.2, 0.3), Dufour number (Du = 0.5, 1.0, 1.5), Soret number (Sr = 0.5, 1.0, 1.5) while the Skin-friction coefficient is increasing, while it is decreasing the values of Magnetic field parameter increases (M = 0.1, 0.3, 0.5), Permeability parameter (K = 0.3, 0.5, 0.7), Maxwell fluid parameter ($\beta$ = 0.2, 0.4, 0.6), Prandtl number (Pr = 0.71, 1.0, 3.0), Chemical reaction parameter (Kr = 0.5, 0.8, 1.2) and Schmidt number (Sc = 0.22, 0.30, 0.60).The numerical values of rate of heat transfer coefficient in terms of Nusselt number are presented in table-3 for various values of Prandtl number (Pr = 0.71, 1.0, 3.0), Thermophoresis parameter (Nt = 0.1, 0.3, 0.5), Brownian motion parameter (Nb = 0.1, 0.2,

0.3), Dufour number (Du = 0.5, 1.0, 1.5). From this table, It has been discovered that as the Thermophoresis parameter is increased, (Nt = 0.1, 0.3, 0.5) the heat transfer coefficientrate is gradually rising, Brownian motion parameter (Nb = 0.1, 0.2, 0.3), Dufour number (Du = 0.5, 1.0, 1.5), while increasing values ofPr have the opposite impact of Prandtl Number Pr (= 0.71, 1.0, 3.0).The effects of parameter of Thermophoresis (Nt = 0.1, 0.3, 0.5), Brownian motion parameter (Nb = 0.1, 0.2, 0.3), Soret number (Sr = 0.5, 1.0, 1.5), Chemical reaction parameter (Kr = 0.5, 0.8, 1.2) and Schmidt number (Sc = 0.22, 0.30, 0.60) Table-4 discusses the rate of mass transfer coefficient or the Sherwood number coefficient. According to this table, the rate of mass transfer coefficient increases as the value of increases Thermophoresis parameter(Nt = 0.1, 0.3, 0.5)and decreasing with increasing values of Brownian motion parameter (Nb= 0.1, 0.2, 0.3) and Schmidt number (Sc= 0.22, 0.30, 0.60).

**Table-2.: coefficient of Skin-friction values for modifications of M,β,K, Du, Sr,Pr, Sc,Nb,Nt, Kr**

| *M* | *β* | *K* | *Du* | *Sr* | Pr | *Sc* | *Nb* | *Nt* | *Kr* | *Cf* |
|---|---|---|---|---|---|---|---|---|---|---|
| 0.1 | 0.2 | 0.3 | 0.5 | 0.5 | 0.71 | 0.22 | 0.1 | 0.1 | 0.5 | 1.866670936130946 |
| **0.3** | | | | | | | | | | 1.824683908634963 |
| **0.5** | | | | | | | | | | 1.804750834601374 |
| | **0.4** | | | | | | | | | 1.838787958719321 |
| | **0.6** | | | | | | | | | 1.793756086107565 |
| | | **0.5** | | | | | | | | 1.841098371349770 |
| | | **0.7** | | | | | | | | 1.829986771383458 |
| | | | **1.0** | | | | | | | 1.880934871346103 |
| | | | **1.5** | | | | | | | 1.906768410971341 |
| | | | | **1.0** | | | | | | 1.872293606407634 |
| | | | | **1.5** | | | | | | 1.896768709873987 |
| | | | | | **1.00** | | | | | 1.823313874513345 |
| | | | | | **3.00** | | | | | 1.797686731093831 |
| | | | | | | **0.30** | | | | 1.832659065109639 |

| | | | | | | | | | | |
|---|---|---|---|---|---|---|---|---|---|---|
| | | | | | | **0.60** | | | | 1.800875207687520 |
| | | | | | | | **0.2** | | | 1.885672098673023 |
| | | | | | | | **0.3** | | | 1.896475630746384 |
| | | | | | | | | **0.3** | | 1.893473134444993 |
| | | | | | | | | **0.5** | | 1.906574986498469 |
| | | | | | | | | | **0.8** | 1.840456209794985 |
| | | | | | | | | | **1.2** | 1.826768736173396 |

**Table-3.: heat transfer coefficient rate (Nusselt number) values for various values of Pr, Du, Nb,Nt**

| Pr | *Du* | *Nb* | *Nt* | *Nu* |
|---|---|---|---|---|
| 0.71 | 0.5 | 0.1 | 0.1 | 0.686916397613946 |
| **1.00** | | | | 0.656398619306109 |
| **3.00** | | | | 0.616874619346331 |
| | **1.0** | | | 0.706787193843716 |
| | **1.5** | | | 0.726786734673461 |
| | | **0.2** | | 0.696768567298407 |
| | | **0.3** | | 0.706785296736903 |
| | | | **0.3** | 0.716786798678676 |
| | | | **0.5** | 0.729875765429429 |

**Table-4.: Rate of mass transfer coefficient (Sherwood number) values for modifications of Sc, Sr, Nb,Nt, Kr**

| *Sc* | *Sr* | *Nb* | *Nt* | *Kr* | *Sh* |
|---|---|---|---|---|---|
| 0.22 | 0.5 | 0.1 | 0.1 | 0.5 | 1.246787390873694 |
| **0.30** | | | | | 1.218678179879863 |
| **0.60** | | | | | 1.181374308530672 |
| | **1.0** | | | | 1.266768769876958 |
| | **1.5** | | | | 1.286758672986742 |
| | | **0.2** | | | 1.220982987498628 |
| | | **0.3** | | | 1.205667096190669 |
| | | | **0.3** | | 1.266798679681791 |
| | | | **0.5** | | 1.286798579856713 |
| | | | | **0.8** | 1.226786578964793 |
| | | | | **1.2** | 1.206786798673982 |

## 6. Conclusions:

In the current research work, the total influences of Thermophoresis, thermal diffusion (Soret) and Dufour (diffusion thermo), Brownian motion two-dimensionally, steady, incompressible, electrically conducting, viscous, fluid of Maxwell move towards a stretching sheet being present nanofluid particles, porous medium, magnetic field and chemical reaction model is investigated. For this investigation, by using method of Runge-Kutta and also with method of shooting technique the resultant governing flow equations are solved. This study paper aims to investigate the effects of M,β,K, Du, Sr,Pr, Sc,Nb,Nt, Kr. on flow variables such as profiles of velocity, temperature, and concentration are all factors to consider as well as coefficients of Skin-friction, rate of heat and mass transfer are studied by graphically and tabular forms. From this investigation, the main findings are:

- By the growing of Magnetic field values the streamwise velocity profiles are decreases and Porous medium The reverse effect is found for Maxwell fluid parameter parameters.

- Decreasing the temperature field due to rising Prandtl number and the opposite values impactis noticed in the event of Thermophoresis, Dufour number and parameter of Brownian motion.
- By increasing in Schmidt number, parameters of Chemical reaction, Brownian motion the concentration profiles is reduced and increased in case of Thermophoresis and Soret parameters.
- Finally, the obtained numerical results are more accurated the reported findings of Makinde and Aziz [36]in a limiting case by taking $M \to 0$, $\beta \to 0$,$Nb \to 0$, $Nt \to 0$, $K \to 0$, $Kr \to 0$,$Sr \to 0$,$Du \to 0$.

**References:**


1. Shojaei A, Amiri A. J., Ardahaie S. S., Hosseinzadeh K, Ganji D. D., Hydrothermal analysis of Non-Newtonian second-grade fluid flow on a radiative stretching cylinder with Soret and Dufour effects. Case Stud. Thermal Eng. 2019;13:100384. doi: 10.1016/j.csite.2018.100384.
2. Bekezhanova, V. B., Goncharova O. N., Influence of the Dufour and Soret effects on the characteristics of evaporating liquid flows. Int. J. Heat Mass Tran. 2020;154:119696.
3. Salleh SNA, Bachok N, Arifin NM, Ali FM. Influence of Soret and Dufour on forced convection flow towards a moving thin needle considering Buongiorno's nanofluid model. Alex Eng. J. 2020;59(5):3897-3906. doi: 10.1016/j.aej.2020.06.045.
4. Jawad M, Saeed A, Kumam P, Shah Z, Khan A. Analysis of boundary layer MHD Darcy-Forchheimer radiative nanofluid flow with Soret and Dufour effects by means of marangoni convection. Case Stud. Therm. Eng. 2021;23:100792. doi: 10.1016/j.csite.2020.100792.
5. Shehzad SA, Abbas Z, Rauf A, Abdelmalek Z. Dynamics of fluid flow through Soret-Dufour impacts subject to upward and downward motion of rotating disk. Int. Commun. Heat Mass. 2021;120:105025. doi: 10.1016/j.icheatmasstransfer.2020.105025.
6. P. O. Olanrewaju, O. D. Makinde, Effects of thermal diffusion and diffusion thermo on chemically reacting MHD boundary layer of flow of heat and mass transfer past a moving vertical plate with suction/injection,Arab J Sci Eng, 36 (2011), pp. 1607-1619.
7. A. Majeed, A. Zeeshan, R. Ellahi, Chemical reaction and heat transfer on boundary layer Maxwell Ferro-fluid flow under magnetic dipole with Soret and suction effects, Eng. Sci. Technol., 20 (3) (2017), pp. 1122-1128.
8. P. S. Reddy, A. J. Chamkha, Soret and Dufour effects on unsteady MHD heat and mass transfer from a permeable stretching sheet with thermophoresis and non-uniform heat generation/absorption,J. Appl. Fluid Mech., 9 (5) (2016), pp. 2443-2455.
9. A. A. Yinusa, M. G. Sobamowo, M. A. Usman, E. H. Abubakar, Exploration of three dimensional squeezed flow and heat transfer through a rotating channel with coupled Dufour and Soret influences, Therm. Sci. Eng. Progr., 21 (2021), Article 100788.
10. S. A. Khan, T. Hayat, A. Alsaedi, Irreversibility analysis in Darcy-Forchheimer flow of viscous fluid with Dufour and Soret effects via finite difference method, Case Stud. Therm. Eng., 26 (2021), T. Hayat, S. Asghar, A. Tanveer, A. Alsaedi, Chemical

reaction in peristaltic motion of MHD couple stress fluid in channel with Soret and Dufour effects, Results Phys., 10 (2018), pp. 69-80.

11. Nuka Venkatesh, M. Anil Kumar and R. Srinivasa Raju, Dufour and Soret influence on MHD boundary layer flow of a Maxwell fluid over a stretching sheet with nanoparticles, Heat Transfer Journal (Wiley Online), https://doi.org/10.1002/htj.22543.
12. Siva Reddy Sheri and R. Srinivasa Raju, Soret effect on unsteady MHD free convective flow past a semi-infinite vertical plate in the presence viscous dissipation, International Journal for Computational Methods in Engineering Science and Mechanics, Vol. 16, Issue 2, pp. 132-141, 2015.
13. J. Anand Rao, P. Ramesh Babu and R. Srinivasa Raju, Finite element analysis of unsteady MHD free convection flow past an infinite vertical plate with Soret, Dufour, Thermal radiation and Heat source, ARPN Journal of Engineering and Applied Sciences, Vol. 10, No. 12, pp. 5338-5351,2015.
14. W. I. A. Okuyade, T. M. Abbey, A. T. Gima-Laabel, Unsteady MHD free convective chemically reacting fluid flows over a vertical plate with thermal radiation, Dufour, Soret, and constant suction effects, Alex. Eng. J., 57 (2018), pp. 3863-3871.
15. S. S. Motsa, S. Shateyi, Successive linearization analysis of the effects of partial slip, thermal diffusion, and diffusion-thermo on steady MHD convective flow due to a rotating disk, Math. Prob. Eng., 2012 (2012), p. 15 pages, 10.1155/2012/397637, Article ID: 397637
16. Humara Sardar, Latif Ahmad, Masood Khan, Ali Saleh Alshomrani, Investigation of mixed convection Carreau nanofluid flow over a wedge in the presence of Soret and Dufour effects, Int. J. Heat Mass Transf., 137 (2019), pp. 809-822.
17. K. Sharada, B. Shankar, Soret and Dufour effects on MHD mixed convection flow of Carreau nanofluid over an exponentially stretching sheet with concentration slip,J. Nanofluids, 6 (6) (2017), pp. 1143-1148.
18. B. Ahmad, A. Perviz, M. O. Ahmad, F. Dayan, Numerical solution with non-polynomial cubic spline technique of order four homogeneous parabolic partial differential equations,Sci. Inq. Rev., 5 (4) (2021).
19. B. Ali, S. Hussain, Y. Nie, A. K. Hussein, D. Habib, Finite element investigation of Dufour and Soret impacts on MHD rotating flow of Oldroyd-B nanofluid over a stretching sheet with double diffusion CattaneoChristov heat flux model, Powder Technol., 377 (2021), pp. 439-452.
20. D. Srinivasacharya, B. Mallikarjuna, R. Bhuvanavijaya, Soret and Dufour effects on mixed convection along a vertical wavy surface in a porous medium with variable properties, Ain Shams Eng. J., 6 (2) (2015), pp. 553-564, 10.1016/j.asej.2014.11.007.
21. Shojaei, A., Amiri, A. J., Ardahaie, S. S., Hosseinzadeh, K. and Ganji, D. D. Hydrothermal analysis of Non-Newtonian second-grade fluid flow on a radiative stretching cylinder with Soret and Dufour effects. Case Stud. Thermal Eng 13, 100384 (2019).
22. Pal, D. and Mondal, H. Influence of thermophoresis and Soret-Dufour on magnetohydrodynamic heat and mass transfer over a nonisothermal wedge with thermal radiation and Ohmic dissipation. J. Magn. Magn. Mater. 331, 250-255 (2013).

23. O. D. Makinde, On MHD mixed convection with Soret and Dufour effects past a vertical plate embedded in a porous plate medium, Latin Amer Appl Res, 41 (2011), pp. 63-68.
24. O. D. Makinde, O. P. Olanrewaju, Unsteady mixedconvection with Soret and Dufour effects past a porous plate moving through a binary mixture of chemically reacting fluid, Chem EngCommun, 198 (7) (2011), pp. 920-938.
25. Aly A.M., Natural convection over circular cylinders in a porous enclosure filled with a nanofluid under thermo-diffusion effects, J. Taiwan Inst. Chem. Eng., 70 (2017), pp. 88-103.
26. Sheremet M.A., The influence of cross effects on the characteristics of heat and mass transfer in the conditions of conjugate natural convection, J. Eng. Thermophys., 19 (3) (2010), pp. 119-127.
27. Arun S., Satheesh A., Mesoscopic analysis of MHD double diffusive natural convection and entropy generation in an enclosure filled with liquid metal, J. Taiwan Inst. Chem. Eng., 95 (2019), pp. 155-173.
28. Chamkha A.J., Al-Naser H., Hydromagnetic double-diffusive convection in a rectangular enclosure with opposing temperature and concentration gradients, Int. J. Heat Mass Transfer, 45 (12) (2002), pp. 2465-2483.
29. J.-T. Hu, S.-J. Mei, Combined thermal and moisture convection and entropy generation in an inclined rectangular enclosure partially saturated with porous wall: nonlinear effects with Soret and Dufour numbers, Int. J. Mech. Sci., 199 (2021), Article 106412.
30. Akolade M.T., Idowu A.S., Adeosun A.T., Multislip and Soret-Dufour influence on nonlinear convection flow of MHD dissipative casson fluid over a slendering stretching sheet with generalized heat flux phenomenon, Heat Transf Res, 50 (5) (2021), pp. 3913-3933.
31. Idowu A.S., Falodun B.O., Variable thermal conductivity and viscosity effects on non-Newtonian fluids flow through a vertical porous plate under soret-dufour influence, Math Comput Simulation, 177 (2020), pp. 358-384.
32. Ali A., Sajjad A., Asghar S., Thermal-diffusion and diffusion-thermo effects in a nanofluid flow with nonuniform heat flux and convective walls, Journal of Nanofluids, 8 (6) (2019), pp. 1367-1372.
33. Akolade M.T., Idowu A.S., Adeosun A.T., Multislip and Soret-Dufour influence on nonlinear convection flow of MHD dissipative casson fluid over a slendering stretching sheet with generalized heat flux phenomenon, Heat Transf Res, 50 (5) (2021), pp. 3913-3933.
34. Layek G., Mandal B., Bhattacharyya K., Dufour and soret effects on unsteady heat and mass transfer for Powell-Eyring fluid flow over an expanding permeable sheet, J Appl Comput Mech, 6 (4) (2020), pp. 985-998.
35. Vafai K., Khan A.A., Fatima G., Sait S.M., Dufour Ellahi R., Soret and radiation effects with magnetic dipole on Powell-Eyring fluid flow over a stretching sheet, Int J Numer Methods, 31 (4) (2021), pp. 1085-1103.
36. O.D. Makinde, A. Aziz, Boundary layer flow of a nanofluid past a stretching sheet with a convective boundary condition, Int. J. Therm. Sci. 50 (2011) 1326-1332.